ISSN 1070-3284, Russian Journal of Coordination Chemistry, 2019, Vol. 45, No. 12, pp. 836–842. © Pleiades Publishing, Ltd., 2019.
Russian Text © The Author(s), 2019, published in Koordinatsionnaya Khimiya, 2019, Vol. 45, No. 12, pp. 713–719.

Solvothermal Synthesis of the Metal-Organic Framework MOF-5 in Autoclaves Prepared by 3D Printing

G. L. Denisov[a], P. V. Primakov[a, b], A. A. Korlyukov[a], V. V. Novikov[a], and Yu. V. Nelyubina[a, c, *]

[a] *Nesmeyanov Institute of Organoelement Compounds, Russian Academy of Sciences, Moscow, 119991 Russia*

[b] *Moscow State University, Moscow, 119992 Russia*

[c] *Kurnakov Institute of General and Inorganic Chemistry, Russian Academy of Sciences, Moscow, 119991 Russia*

**e-mail: unelya@ineos.ac.ru*

Received June 24, 2019; revised July 10, 2019; accepted July 22, 2019

Abstract—The known metal-organic framework $\{Zn_4O(BDC)_3\}$ (MOF-5 (**I**), where BDC is terephthalate anion) is synthesized by the solvothermal method in autoclaves prepared by 3D printing from polypropylene. The synthesized polymer is isolated in the individual state and characterized by elemental analysis and powder X-ray diffraction analysis. The crystal structures of MOF-5 and another coordination polymer based on zinc(II) terephthalate $\{Zn_4O(BDC)_3\} \cdot (ZnO)_{0.125}$ (SUMOF-2 (**II**)) obtained as a by-product of the solvothermal synthesis are confirmed by X-ray diffraction analysis (CIF files CCDC nos. 1920366 (**I**) and 1926136 (**II**)).

Keywords: 3D printing, autoclave, metal-organic framework, X-ray diffraction analysis, solvothermal synthesis, zinc terephthalate

DOI: 10.1134/S1070328419120030

INTRODUCTION

Mesoporous metal-organic frameworks (MOF) [1] in which the three-dimensional crystal structure is formed by metal-containing nodes linked by strong chemical bonds with organic linkages [2] are objects of rapt attention and investigation of specialists working in various areas of science and industry [3]. Owing to their unique properties (high internal surface area, low density, and thermal stability [4] and the possibility to vary the pore size [2]), they found wide use for gas storage [5] and separation [6], as proton-conducting membranes [7] and catalysts or their "containers" in diverse chemical processes [8], for targeted drug delivery [9], and even for determining structures of biomacromolecules [10]. There are many various approaches to the synthesis of new MOF [11]. However, single crystals of good quality necessary to determine their structure by the X-ray diffraction method can be obtained only under the solvothermal conditions [12]. In this case, the initial organic and inorganic components are heated with a highly boiling polar solvent to temperatures exceeding the boiling point of the chosen solvent [13] in expensive metallic autoclaves of a specified volume. The technology of additive 3D printing [14] of polypropylene autoclaves with the necessary chemical and thermal stability [15] has recently been proposed to use for the synthesis of MOF.

In the recent time, 3D printing for the preparation of monolithic plastic units by the multilayer extrusion of a molten polymer based on the digital three-dimensional model [14] is used in chemistry for the production of the cheap scientific equipment that can be adjusted to researcher's needs [16–18] and for manufacturing vessels for chemical reactions [14, 15, 19, 20]. Since these units are cheap and desirable characteristics (external sizes and shapes, wall thickness, internal volume, etc.) can be imparted to them, they provide wide possibilities for the solvothermal synthesis of MOF. For example, the use of this approach for various combinations of metal-containing nodes and organic linkages (pyridine and carboxylic acids) allowed two new MOF to be found, and the synthesis conditions for one of them were optimized [15].

In this work, we synthesized the well known MOF based on zinc(II) terephthalate $\{Zn_4O(BDC)_3\}$ (MOF-5, **I**), where BDC is terephthalate anion [4], under the solvothermal synthesis conditions, in the autoclaves prepared from polypropylene by 3D printing (Fig. 1). Complex **I** was isolated in the individual state and characterized by elemental analysis and powder X-ray diffraction analysis. The structure of another MOF $\{Zn_4O(BDC)_3\} \cdot (ZnO)_{0.125}$ (SUMOF-2, **II**), which was obtained as a by-product under the same conditions in the initial stages of optimization of the parameters of the polypropylene autoclaves for the

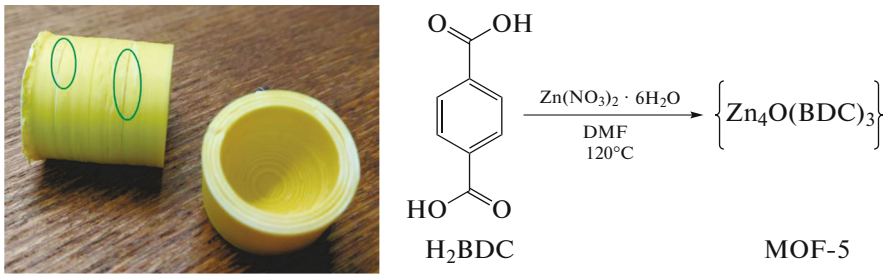

Fig. 1. Polypropylene autoclave cut with a dremel and the scheme for the solvothermal synthesis of MOF **I**. The cracks formed in the autoclave with a wall thickness of 4 mm upon storage at 120°C for 16 h are green-colored.

solvothermal synthesis, was also confirmed by X-ray diffraction analysis.

EXPERIMENTAL

All procedures on the synthesis of the complexes were carried out in air using commercially available organic solvents and reagents. Analyses to carbon and hydrogen were conducted on a CarloErba microanalyzer (model 1106). Complex **I** was synthesized using a previously described procedure [21].

Synthesis of MOF I. Weighed samples of $Zn(NO_3)_2 \cdot 6H_2O$ (47.52 mg, 0.1597 mmol) and H_2BDC (8.71 mg, 0.0524 mmol) were dissolved or suspended in anhydrous dimethylformamide (DMF) (1.34 mL) to form a transparent solution. The reaction mixture was placed in the 2.2-mL autoclave prepared by 80% using the additive 3D printing technology [15] after which printing was continued to the entire sealing of the autoclave achieved in 4 h. The autoclave with the reaction mixture (61% of the volume were filled [15]) was heated to 120°C in a drying box with programed heating–cooling cycles and kept at this temperature for 16 h. After cooling to room temperature, the autoclave was opened by cutting it in parallel to polypropylene layers at a height of ~8 mm from the upper boundary using a dremel with a circulation nozzle (Fig. 1a). The crystalline product obtained in the autoclave as transparent cubic single crystals suitable for X-ray diffraction analysis was separated from the mother liquor and washed in DMF (5 mL) for 24 h. A similar procedure was repeated two times in $CHCl_3$ (5 mL) followed by drying on a rotary evaporator at room temperature for 2 h. The yield of the product was 29.5 mg (25%).

For $C_{24}H_{12}O_{13}Zn_4$		
Anal. calcd., %	C, 37.44	H, 1.57
Found, %	C, 37.32	H, 1.73

Synthesis of MOF II was similar to the synthesis of MOF **I**. The obtained crystalline product in the form of transparent cubic single crystals was not isolated in the individual state, and its composition and structure were determined by the powder X-ray diffraction method and X-ray diffraction analysis.

X-ray diffraction analyses of the single crystals of MOF **I** and **II** taken from the autoclaves immediately after cooling and opening were carried out at 120 K on a Bruker APEX2 DUO CCD diffractometer (MoK_α radiation, graphite monochromator, ω scan mode). The structures were solved by a direct method and refined by least squares in the anisotropic full-matrix approximation for F^2_{hkl}. The positions of the hydrogen atoms calculated geometrically were refined in the isotropic approximation by the riding model. The guest DMF molecules in the cavities of the structures of compounds **I** and **II** are strongly disordered and cannot be refined as a set of discrete positions. The SQUEEZE/PLATON procedure [22] was applied to take them into account as a diffuse contribution to the total scattering of the crystal. Selected crystallographic data and refinement parameters for the structures of MOF **I** and **II** are presented in Table 1. All calculations were performed using the SHELXTL PLUS [23] and Olex2 [24] programs.

The full sets of X-ray diffraction data for compounds **I** and **II** were deposited with the Cambridge Crystallographic Data Centre (CIF files CCDC nos. 1920366 and 1926136, respectively; http://www.ccdc.cam.ac.uk/).

Powder X-ray diffraction method. The powder X-ray diffraction patterns of the obtained purified and dried powders were measured on a Bruker D8 Advance diffractometer equipped with a Ge(111) focusing monochromator ($\lambda(CuK_{\alpha 1}) = 1.5406$ Å) and a LynxEye linear positional-sensitive detector in the transmission geometry in the angle range $2\theta = 7°–60°$. All calculations were performed using the TOPAS 4.21 program [25].

Preparation of autoclaves. Engineering polypropylene FL-33 (yellow) with the softening point 160°C [15] was used as a material for the preparation of the autoclaves by 3D printing methods (Fig. 1) and purchased at top3Dshop [26] as a standard bobbin for 3D printing with a coiled polypropylene rod 1.75 mm in diameter. This material is characterized by the neces-

Table 1. Selected crystallographic data and refinement parameters for compounds **I** and **II**

Parameter	Value	
	I	**II**
Empirical formula	$C_{24}H_{12}O_{13}Zn_4$	$C_{16}H_8O_{8.7}Zn_{2.75}$
FW	769.90	520.05
Crystal system	Cubic	Trigonal
Space group	*Fm-3m*	*R-3*
Z	8	18
a, Å	25.89(2)	18.4128(11)
c, Å	25.89(2)	43.8686(19)
V, Å^3	1737(4)	1288(1)
ρ_{calc}, g cm^{-3}	0.590	1.207
μ, cm^{-1}	1.113	2.318
F(000)	3040	4635
$2\theta_{max}$, deg	55	54
Number of measured reflections	46031	59662
Number of independent reflections	1057	6259
Number of reflections with $I > 2\sigma(I)$	442	4016
Number of refined parameters	25	282
R_1 (for reflections with $I > 2\sigma(I)$)	0.0586	0.0587
wR_2 (for all reflections)	0.2811	0.2073
GOOF	1.237	1.0591
Residual electron density, e Å^{-3}	−1.162/0.604	−1.926/1.576

sary thermal and chemical resistance to various solvents and reagents [15] under the solvothermal conditions for the synthesis of metal-organic frameworks (120°C, DMF). The free OpenSCAD software [27] was applied for the parametric simulation of the autoclave, and the three-dimensional model obtained in the STL format [28] was transformed into the GCODE machine format [29] for subsequent 3D printing using the Simplify3D program [30]. The printing was carried out on the commercial Magnum Creative 2 UNI 3D printer [31] at the temperature of the jet 248°C and the printing speed not higher than 750 mm/min. A polypropylene board 5 mm thick was used as a support. The wall thickness of the 2.2-mL autoclave was chosen to range from 4 to 6 mm.

RESULTS AND DISCUSSION

The solvothermal synthesis of MOF **I** was carried out using a previously described procedure [21] including the dissolution of $Zn(NO_3)_2 \cdot 6H_2O$ and H_2BDC in a molar ratio of 3 : 1 in DMF (Fig. 1) and storage of the reaction mixture at 120°C for 16 h in the autoclave followed by cooling and characterization of the obtained crystalline product by powder X-ray diffraction analysis. The 3D printing parameters by polypropylene (concentrated external layers and internal filling of the snake type) and the autoclave geometry (cylinder with a spherical external cavity and the thickness of all walls equal to 4 mm) optimized for the conditions of the solvothermal synthesis of MOF in DMF at 120°C [15] were used to prepare the polypropylene autoclave. The 3D printing was stopped when the autoclave was prepared by 80%, the reaction mixture was loaded, and the printing was continued to the complete sealing of the autoclave [15].

Under the chosen conditions, the solvothermal synthesis of MOF **I** in thus prepared polypropylene autoclave (Fig. 1) gave a mixture of transparent cubic crystals of two types differed in size. According to the X-ray diffraction data, they represented the MOF based on zinc(II) terephthalate: MOF **I** [1] and **II** [32].

The crystals of compound **I** (Figs. 2, 3) taken from the autoclave immediately after the reaction mixture was cooled to room temperature represented solvates with DMF. As it is characteristic of compound **I** and the whole family of coordination polymers isoreticular to MOF **I** [2], the nodes are the tetrahedral clusters Zn_4O^{6+} with the Zn^{2+} ions at the vertices of the tetrahedron (Zn···Zn 3.160(3) Å) linked to the O^{2-} anion at the center (Zn–O 1.9350(13) Å). The presence of the O^{2-} anion is a result, most likely, of the partial decom-

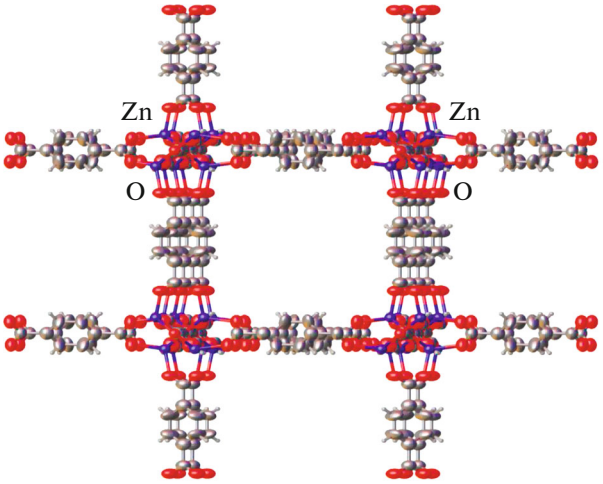

Fig. 2. Fragment of the crystal packing of MOF **I** in the representation of atoms by thermal vibration ellipsoids (p = 30%). Hydrogen atoms and disordered guest DMF molecules are omitted for clarity.

position of DMF under the solvothermal synthesis conditions [33]. The Zn_4O^{6+} tetrahedra are bound to each other into a three-dimensional cubic framework by the BDC^{2-} anions (Zn–O 1.945(8) Å) to form large spherical pores with a volume of 1838.78 Å^3 accessible for the solvent (according to an analysis of the obtained X-ray diffraction data using the OLEX2 program [24]). In the crystals of MOF **I** taken from the polypropylene autoclave immediately after cooling to room temperature, the pores are occupied by guest DMF molecules. They were described as a diffuse contribution using the SQUEEZE/PLATON procedure [22] because of strong disordering.

As follows from the data of X-ray diffraction analysis conducted at 120 K, the crystals of the second type correspond to MOF **II** [32], which is similar by crystal structure to "mutually grown" MOF **I** [1]. However, one of two types of pores in MOF **II** is occupied by zinc oxide ZnO (Figs. 3, 4), which connects similar tetrahedra Zn_4O^{6+} localized in the nodes of the three-dimensional framework (Zn···Zn 3.162(1)–3.2303(10) Å, Zn–O 1.934(2)–1.984(6) Å) between each other (Zn–O 2.33(4) Å) in addition to the BDC^{2-} anions that serve as linkages (Zn–O 1.899(5)–1.980(13) Å). The estimated [24] volume of the largest spherical pore accessible for the solvent is 195.43 Å^3. In the crystals of MOF **II** formed in the polypropylene autoclave during the solvothermal synthesis of MOF **I**, the pores are occupied by disordered DMF molecules, which were also described as a diffuse contribution without refining certain atomic positions using the SQUEEZE/PLATON procedure [22].

The presence of two crystalline phases corresponding to MOF **I** and **II** was confirmed by powder X-ray diffraction analysis at room temperature (Fig. 5) in the subsequent study of the obtained mixture of crystals after washing and drying to remove the residual solvent using the previously proposed scheme [21].

The reason for the formation of a mixture of two MOF based on zinc(II) terephthalate instead of indi-

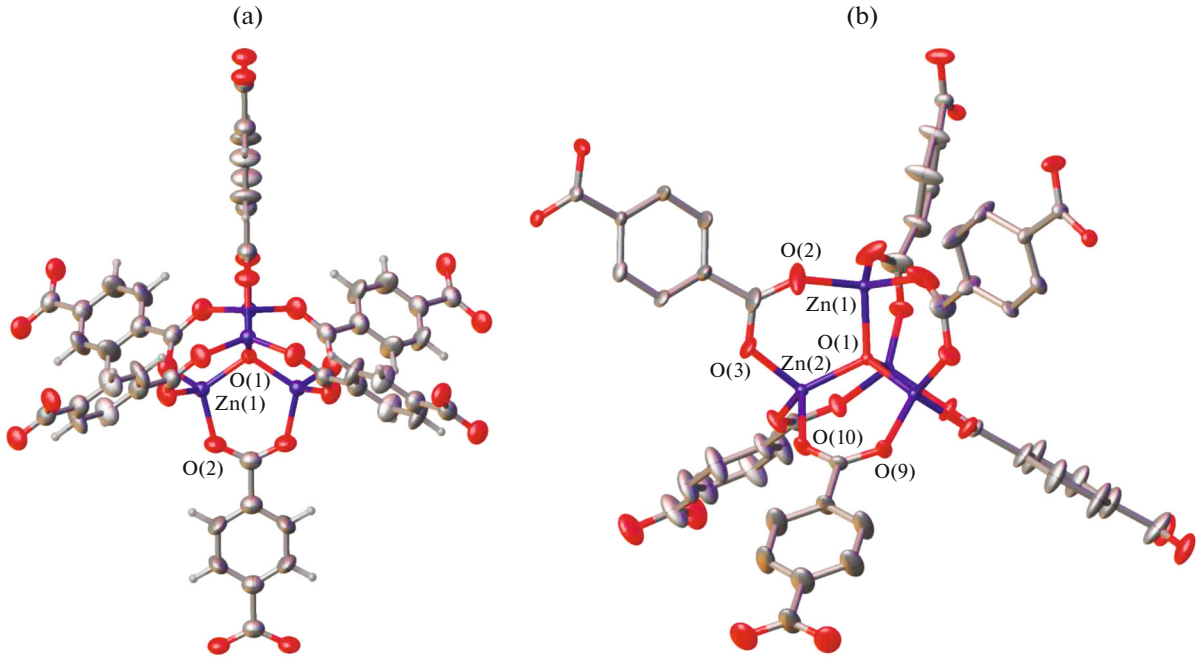

Fig. 3. General view of the "nodes" in the crystals of MOF (a) **I** and (b) **II** in the representation of atoms by thermal vibration ellipsoids (p = 30%). Hydrogen atoms and disordered guest DMF molecules are omitted for clarity.

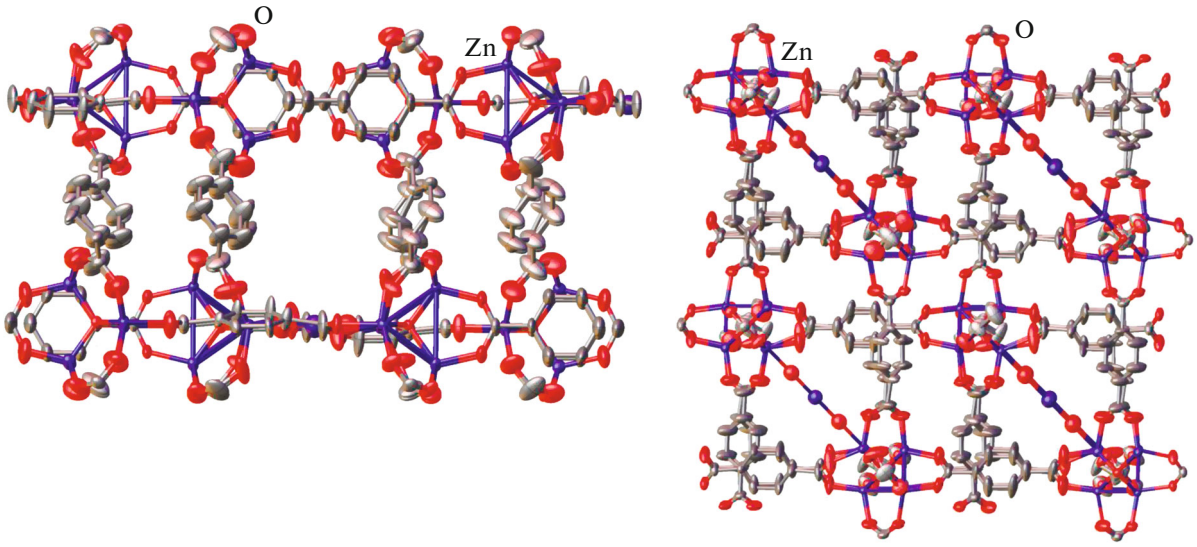

Fig. 4. Fragments of the crystal packing of MOF **II** in the representation of atoms by thermal vibration ellipsoids (p = 30%). Hydrogen atoms are omitted for clarity.

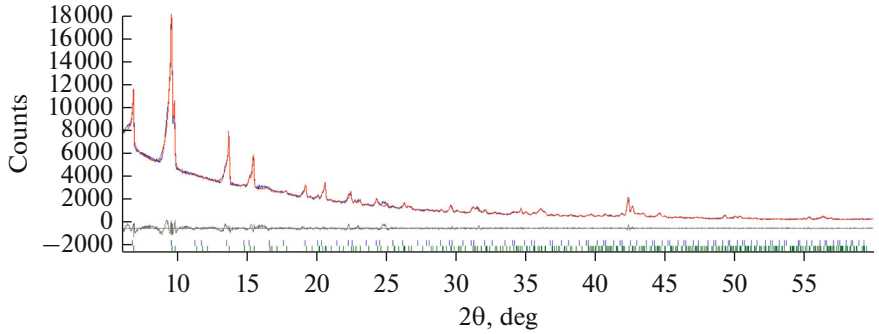

Fig. 5. Diffraction pattern of the crystalline powder containing MOF **I** and **II**: (1, 2) joint experimental (blue) and calculated (red) curves and (3) the difference between the experiment and calculation for a mixture of MOF **I** and **II** (gray).

vidual MOF **I** expected to form under the solvothermal synthesis conditions (120°C, DMF) was found due to the careful study of the polypropylene autoclave used for the synthesis. Although similar [15] cylindrical autoclaves with a wall thickness of 4 mm sustained the pressure created during the solvothermal synthesis of MOF, cracks between polypropylene layers observed by the naked eye appeared on the external wall of the prepared autoclave after prolong storage at 120°C (Fig. 1a). This can be related to the fact that the softening temperature of polypropylene purchased from different producers often differ (130–160°C), as well as the optimal parameters of 3D printing by multilayer extrusion (flow rate of the polypropylene rod, extrusion multiplier, temperature of the nozzle, etc.).

To eliminate the arisen problem of an impermeability of the autoclave that led to leaking of the solution through the formed cracks (as followed from a noticeable decrease in the weight of the autoclave compared to the initial weight), we proposed to increase the wall thickness from 4 to 6 mm remaining other parameters, i.e., the shape and volume of the internal cavity (2.2 mL), unchanged. The mechanical strength of the modified model of the autoclave was tested under similar solvothermal conditions (120°C, DMF) but in the absence of the initial organic (H_2BDC) and inorganic ($Zn(NO_3)_2 \cdot 6H_2O$) components. In this case, the difference in the weights of the autoclave before and after heating of the pure solvent was lower than 0.1%.

The solvothermal synthesis of MOF **I** under the same conditions in the modified polypropylene autoclave (without visible cracks on its external side or without an appreciable change in the weight) gave the target MOF in a yield of 25% comparable with the yield in the synthesis without using autoclaves pre-

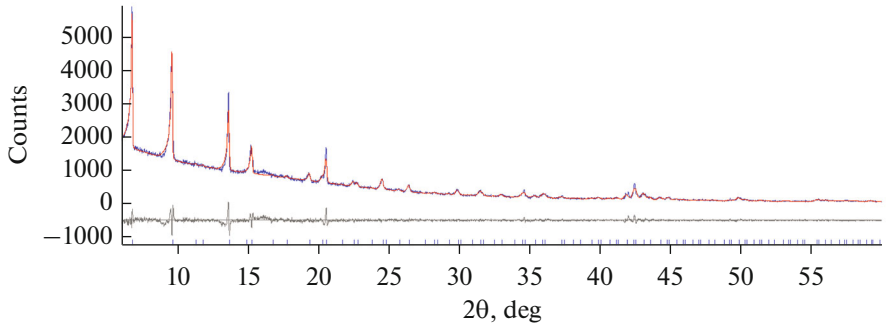

Fig. 6. Diffraction pattern of the crystalline powder containing pure MOF **I**: (1, 2) joint experimental (blue) and calculated (red) curves and (3) the difference between the experiment and calculation (gray).

pared by the 3D printing technology (e.g., 28.8% [21]). Prepared MOF **I** was isolated in the individual state and characterized by elemental analysis and powder X-ray diffraction analysis at room temperature (Fig. 6). The corresponding diffraction pattern was indexed in the cubic crystal system with the unit cell parameter $a = 25.84$ Å, which closely reproduces the X-ray diffraction analysis results of a single crystal of MOF **I** at 120 K (Table 1). The average size of the crystallites in the sample purified from the residual solvent was estimated from the integral broadening of the diffraction maxima and turned out to be 807 nm.

Thus, we obtained MOF **I** by the solvothermal synthesis in the autoclaves prepared from polypropylene using the additive 3D printing technology (Fig. 1). The composition and structure of MOF-5 were confirmed by elemental analysis and powder X-ray diffraction analysis. Large single crystals obtained due to this approach under the solvothermal conditions were of good quality and also allowed us to unambiguously determine the structure of MOF **I** by the X-ray diffraction method.

The use of polypropylene autoclaves for this purpose makes it possible to carry out solvothermal synthesis in an almost infinite number of identical autoclaves, the cost of the preparation of which is equal of the cost of the chosen material. These autoclaves have specified characteristics that can be changed according to the wish of researchers. This provides wide possibilities for the search for new MOF and optimization of conditions for their preparation depending on various parameters (concentrations of the initial reagents, solvent nature, temperature, pressure, reaction time, and cooling rate [12]), which determine, to a significant extent, the properties of the final product [34] and prospects of its practical use.

ACKNOWLEDGMENTS

The structures of the synthesized compounds were studied using the equipment of the Center of Molecular Structure Investigation at the Nesmeyanov Institute of Organoelement Compounds (Russian Academy of Sciences) and supported by the Ministry of Science and Higher Education of the Russian Federation.

FUNDING

This work was supported by the Russian Foundation for Basic Research, project no. 18-29-04020.

CONFLICT OF INTEREST

The authors declare that they have no conflicts of interest.

REFERENCES

1. Yaghi, O. and Li, H., *J. Am. Chem. Soc.*, 1995, vol. 117, no. 41, p. 10401.
2. Yaghi, O.M., O'Keeffe, M., Ockwig, N.W., et al., *Nature*, 2003, vol. 423, no. 6941, p. 705.
3. Peplow, M., *Nature News*, 2015, vol. 520, no. 7546, p. 148.
4. Li, H., Eddaoudi, M., O'Keeffe, M., and Yaghi, O.M., *Nature*, 1999, vol. 402, no. 6759, p. 276.
5. Wilmer, C.E., Leaf, M., Lee, C.Y., et al., *Nature Chemistry*, 2012, vol. 4, no. 2, p. 83.
6. Herm, Z.R., Wiers, B.M., Mason, J.A., et al., *Science*, 2013, vol. 340, no. 6135, p. 960.
7. Yoon, M., Suh, K., Natarajan, S., and Kim, K., *Angew. Chem., Int. Ed. Engl.*, 2013, vol. 52, no. 10, p. 2688.
8. Lee, J., Farha, O.K., Roberts, J., et al., *Chem. Soc. Rev.*, 2009, vol. 38, no. 5, p. 1450.
9. Giménez-Marqués, M., Hidalgo, T., Serre, C., and Horcajada, P., *Coord. Chem. Rev.*, 2016, vol. 307, p. 342.
10. Inokuma, Y., Yoshioka, S., Ariyoshi, J., et al., *Nature*, 2013, vol. 495, no. 7442, p. 461.
11. Stock, N. and Biswas, S., *Chem. Rev.*, 2011, vol. 112, no. 2, pp. 933–969.
12. Zhao, Y., Li, K., and Li, J., *Z. Naturforsch., B: J. Chem. Sci.*, 2010, vol. 65, no. 8, p. 976.
13. Chen, X.-M. and Tong, M.-L., *Acc. Chem. Res.*, 2007, vol. 40, no. 2, p. 162.
14. Gordeev, E., Degtyareva, E., and Ananikov, V., *Izv. Akad. Nauk, Ser. Khim.*, 2016, no. 6, p. 1637.

15. Kitson, P.J., Marshall, R.J., Long, D., et al., *Angew. Chem., Int. Ed. Engl.*, 2014, vol. 53, no. 47, p. 12723.
16. Zhang, C., Wijnen, B., and Pearce, J.M., *J. Lab. Autom.*, 2016, vol. 21, no. 4, p. 517.
17. Baden, T., Chagas, A.M., and Gage, G., *PLoS Biol.*, 2015, vol. 13, no. 3. e1002086.
18. Berman, B., *Business Horizons*, 2012, vol. 55, no. 2, p. 155.
19. Kitson, P.J., Glatzel, S., Chen, W., et al., *Nat. Protocols*, 2016, vol. 11, no. 5, p. 920.
20. Symes, M.D., Kitson, P.J., Yan, J., et al., *Nat. Chem.*, 2012, vol. 4, no. 5, p. 349.
21. Mulyati, T.A., Ediati, R., and Rosyidah, A., *Indones. J. Chem.*, 2015, vol. 15, no. 2, p. 101.
22. Spek, A., *J. Appl. Crystallogr.*, 2003, vol. 36, no. 1, p. 7.
23. Sheldrick, G.M., *Acta Crystallogr., Sect. A: Found. Crystalogr.*, 2008, vol. 64, no. 1, p. 112.
24. Bourhis, L.J., Dolomanov, O.V., Gildea, R.J., et al., *Acta Crystallogr., Sect. A: Found. Adv.*, 2015, vol. 71, no. 1, p. 59.
25. Coelho, A., *Bruker AXS GmbH*, Karlsruhe, 2009.
26. Top3DShop. https://top3dshop.ru/.
27. OpenSCAD. http://www.openscad.org/documentation.html2009.
28. Koc, B., Ma, Y., and Lee, Y.-S., *Rapid Prototyping J.*, 2000, vol. 6, no. 3, p. 186.
29. Smid, P., *CNC Control Setup for Milling and Turning: Mastering CNC Control Systems*, Industrial Press Inc., 2010.
30. Simplify 3D. http://www.simplify3d.com/software/documentation/.
31. Magnum 3D. https://magnum3d.ru/magnum-creative-2-uni/.
32. Yao, Q., Su, J., Cheung, O., et al., *J. Mater. Chem.*, 2012, vol. 22, no. 20, p. 10345.
33. Czaja, A.U., Trukhan, N., and Muller, U., *Chem. Soc. Rev.*, 2009, vol. 38, no. 5, p. 1284.
34. Seetharaj, R., Vandana, P., Arya, P., and Mathew, S., *Arabian J. Chem.*, 2019, vol. 12, no. 3, p. 295.

Translated by E. Yablonskaya